

RESEARCH PAPER

Electrochemical Determination of Gallic Acid in *Camellia sinensis* (L.) Kuntze, *Viola odorata* L., *Commiphora wightii* (Arn.) Bhandari, and *Vitex agnus-castus* L. by MWCNTs-COOH Modified CPE

Sheida Sarafraz¹, Hossain-Ali Rafiee-Pour^{2,*}, Maryam Khayatkashani³ and Asa Ebrahimi¹

¹ Department of Biotechnology, Science and Research branch, Islamic Azad University, Tehran, Iran

² Department of Cell and Molecular Biology, Faculty of Chemistry, University of Kashan, Kashan, Iran

³ School of Traditional Medicine, Tehran University of Medical Sciences, Tehran, Iran

ARTICLE INFO ABSTRACT

Article History:

Received 08 January 2019

Accepted 21 March 2019

Published 01 April 2019

Keywords:

Antioxidant Capacity
Carbon Paste Electrode
Electrochemical Sensor
Gallic Acid
Multiwalled Carbon
Nanotubes
Plants Extracts

Gallic acid (GA) is the main phenolic antioxidant which has been subjected of many studies because of its important biological properties including anticancer, anti-inflammatory and antimicrobial activities as well as free radicals scavenger and cardiovascular diseases protector. Hereupon, fabricating a selective and sensitive sensor for GA detection and measurement is an important issue. In this paper, a carboxylated MWCNTs modified carbon paste electrode (MWCNTs-COOH/CPE) was successfully fabricated and employed for GA determination. Activating the carboxylic sites of the MWCNTs carried out in nitric acid solution in an ultrasonic bath and further studied by field emission scanning electron microscopy (FESEM), X-ray diffraction (XRD) and Fourier transform infrared (FTIR) spectroscopy. The electrocatalytic oxidation of GA at the MWCNTs-COOH/CPE surface was studied by cyclic voltammetry (CV) and differential pulse voltammetry (DPV) methods. The GA presented a high electrochemical response on MWCNTs-COOH/CPE at pH 2 in comparison with the CPE. This sensor showed a linear response range of 0.33 - 196 μM and a detection limit of 17.2 nM (S/N = 3). Furthermore, the designed MWCNTs-COOH/CPE was successfully applied as an electrochemical sensing system for GA determination in extracts of *Camellia sinensis* (L.) Kuntze, *Viola odorata* L., *Commiphora wightii* (Arn.) Bhandari, and *Vitex agnus-castus* L., with the estimated amount of 11.4, 8.9, 11.91 and 2.9 mg L⁻¹ GA in each plant extract, respectively.

How to cite this article

NAME N. Electrochemical Determination of Gallic Acid in *Camellia sinensis* (L.) Kuntze, *Viola odorata* L., *Commiphora wightii* (Arn.) Bhandari, and *Vitex agnus-castus* L. by MWCNTs-COOH Modified CPE. J Nanostruct, 2019; 9(2): 384-395.
DOI: 10.22052/JNS.2019.02.020

INTRODUCTION

Free radicals are generally reactive oxygen species (ROS) which at high concentration will induce oxidative stress and injure cell structures such as lipids, proteins, and DNAs [1]. Also, they are important in the development of many auto-immune and neurodegenerative diseases, cardiovascular malfunction, cancers, cataracts, aging and rheumatism which seriously threaten human health. Antioxidants could prevent, delay and repair damages caused by ROS through inhibiting the propagation of free radical reactions [2].

* Corresponding Author Email: rafieepour@kashanu.ac.ir

Gallic acid (3, 4, 5-trihydroxybenzoic acid; GA) is the most important phenolic antioxidant which acts as reducing agent, hydrogen donor and singlet oxygen quencher [3] and owes antimicrobial, anti-inflammatory, antimutagenic and anticarcinogenic activities. GA present in fruits, nuts, grapes, and plants [4] such as *Camellia sinensis* (L.) Kuntze (*C. sinensis*) [5], *Viola odorata* L. (*V. odorata*) [6], *Commiphora wightii* (Arn.) Bhandari (*C. wightii*) [7] and *Vitex agnus-castus* L. [8]. Also, GA is used as a reference-standard for total polyphenol content estimation [9].

C. sinensis (green tea) native to China and Southeast Asia is kind of flowering plants of *Theaceae* family. Several studies have shown that green tea confer significant protection against Parkinson's, alzheimer and cancer [10], reduce high cholesterol [11], owing antidiabetic effects [12], antibacterial [13], anti-inflammatory [14], anti-HIV [15] and antioxidant activities [16]. Most methods used for GA detection in *C. sinensis* are electrochemical [17] and HPLC [18].

V. odorata (sweet violet) from *Violaceae* family is native to Europe and Asia. It has been used to remedy hypertension, anxiety, and insomnia [19]. This plant also has diuretic, laxative [20], antibacterial [21], lung-protective [22] and high antioxidant activities [23]. To the best of our knowledge, there is no report of the electrochemical method for GA detection in *V. odorata*. Gontova et al. published an HPLC method in order to quantify phenolic capacity of *V. odorata* [24].

C. wightii (*Commiphora mukul*) known as Indian bdellium-tree is a flowering plant in the family *Burseraceae*. It could be found in Northern Africa to Central Asia, but is most common in Northern India. It is known to have antioxidant [25], and anti-inflammatory [26] activities. Also, it is used as a natural treatment for heart diseases [27]. Muguli et al. used HPLC method for determination of GA in *C. wightii* [28], as we know there is not electrochemical report on GA determination.

V. agnus-castus also called *Vitex* is native to Mediterranean Europe and Central Asia region. It is a medicinal plant contained *flavonoids* [29]. *Vitex*'s fruits and leaves have been shown antioxidant [30], antimicrobial [31] and anti-inflammatory [32] activities. Sarikurkcu et al. used GC-MS method for study antioxidant activity of *V. agnus-castus* [33]. Also, we have not found an electrochemical method determining GA in this plant.

In recent years, several methods have been used for determination of GA and its derivatives include high performance liquid chromatography (HPLC) [34], mass spectrometry [35], flow injection analysis [36], resonance light scattering [37] and capillary zone electrophoresis [38]. These methods require expensive equipment need expensive equipment, complicated function, and toxic organic solvents usage, lead to limit of their application. In contrast, there is an increasing interest on electrochemical methods [39] based on modified electrodes as sensitive,

selective and low-cost analytical techniques for phenolic compound detection and various types of nanostructures have been used as surface modifiers [40-42]. Among the modifiers of the electrode surface, MWCNTs due to unique electronic, thermal and mechanical properties are most commonly used in biomedical and engineering applications [43]. But, MWCNTs have poor solubility in a large number of solvents. The defects on MWCNTs created by oxidants can be stabilized by bonding with carboxylic or hydroxyl groups, which help to stabilize the aqueous MWCNTs-COOH suspension [44].

In this study, we report an electrochemical sensor for rapid determination of GA in plants extracts, using differential pulse voltammetric (DPV) technique based on a carbon paste electrode modified with carboxylated multi-walled carbon nanotubes (MWCNTs-COOH/CPE). The MWCNTs-COOH significantly improves the oxidation peak current of GA.

MATERIALS AND METHODS

Gallic acid was purchased from Sigma-Aldrich. MWCNTs, (diameter: 30-50 nm; length 20 μm) were purchased from Times nano Co. (Chengdu, China) with 95% purity. Pure fine graphite powder and paraffin oil (Merck, Germany) used as binding agents in graphite pastes. Ethanol ($\geq 99.9\%$) and nitric acid (65%) were purchased from the Merck. Dipotassium hydrogen phosphate and potassium dihydrogen phosphate, from Merck, were used to prepare phosphate buffer solution (PBS) with a concentration of 0.2 M and different pH values (2.0 to 5.0) which used as the supporting electrolyte for electrochemical quantification. All aqueous solutions were prepared in doubly distilled water. The extracts of *V. odorata* and *C. wightii* were purchased from the traditional medicine department of Barij Essence Pharmaceutical in Kashan, Iran. Pills of *V. agnus-castus* obtained from Pursina Pharmaceutical Company in Tehran, Iran. *C. sinensis* tea bag received from Lipton Company in Qazvin, Iran. All the other used chemicals and reagents were of analytical grade.

Apparatus

Electrochemical measurements were performed using a computerized potentiostat/galvanostat (model SAMA 500, Isfahan, Iran), and conventional three-electrode system with the modified carbon paste as the working electrode, a platinum rod as

the auxiliary electrode, and a saturated Ag/AgCl electrode as the reference electrode. The used electrochemical techniques are cyclic voltammetry (CV) and differential pulse voltammetry (DPV). IR spectra were determined on a Nicolet Magna series FTIR 550 spectrometer using KBr pellets in the range of 400-4000 cm^{-1} . The XRD patterns were obtained from a diffractometer of Philips Company equipped with a Cu K α anode ($\lambda=1.54 \text{ \AA}$) in the 2θ range from 10 to 80°. The field emission scanning electron microscopy (FESEM) images of the electrode surface were recorded using an electronic microscope (ZEISS, Sigma VP-500, Germany). Other instruments such as water bath ultrasonic (model Eurosonic 4D, Euronda, Montecchio Pre-calcino (Vincenza), Italy) and vacuum filtration system (mixed cellulose ester membrane filter with a pore size of 0.45 μm) were employed in this research.

Carboxylation of MWCNTs

MWCNTs-COOH was prepared using the reported method by Karimi et al. [45]. In brief, 20 mg of MWCNTs was added to 30 mL nitric acid solution (35%) and then ultrasonicated at 40 °C for 6 h which was periodically relaxed for at least 10 min after each 20 min sonication. After that, the black suspension was filtered with vacuum filtration equipped with mixed cellulose ester membrane filter and washed thoroughly with distilled water until neutral pH achieved. The residue dried under the infrared lamp.

Preparation of the MWCNTs-COOH/CPE

MWCNTs-COOH/CPE was prepared by a simple procedure, first 0.004 g of the MWCNTs-COOH were dispersed in 2 ml ethanol using an ultrasonic bath over 10 minutes, then 0.5 g of graphite powder added to the mixture and after drying at room temperature, 6 drops of paraffin oil added, and resultant paste packed into a syringe (2 mm diameter and 10 mm deep). Electrical contact was made by pushing a copper wire through the center of the back mixture. In order to achieve a new surface, CPE surface vertically polished on a piece of waxed paper.

Sample preparation

In order to prepare extracts, 0.25 g of *V. agnus-castus* powder added to 20.0 mL of doubly distilled water:ethanol (30:70) at 25 °C. Also, aqueous *V. odorat*, *C. wightii*, and *C. sinensis* diluted (20x) with doubly distilled water:ethanol (30:70) at 25 °C. Samples subject at ultrasound treatment at a constant frequency of 35 kHz for 30 min at room temperature. The solutions were filtered through a Whatman no. 1 filter paper into a 25 mL volumetric flask and were kept at 4 °C for further use.

RESULTS AND DISCUSSION

Characterization of MWCNTs-COOH

In order to investigate the surface functional groups formed on MWCNTs, FTIR spectra of pristine MWCNTs (Fig. 1-A) and MWCNTs-COOH (Fig. 1-B)

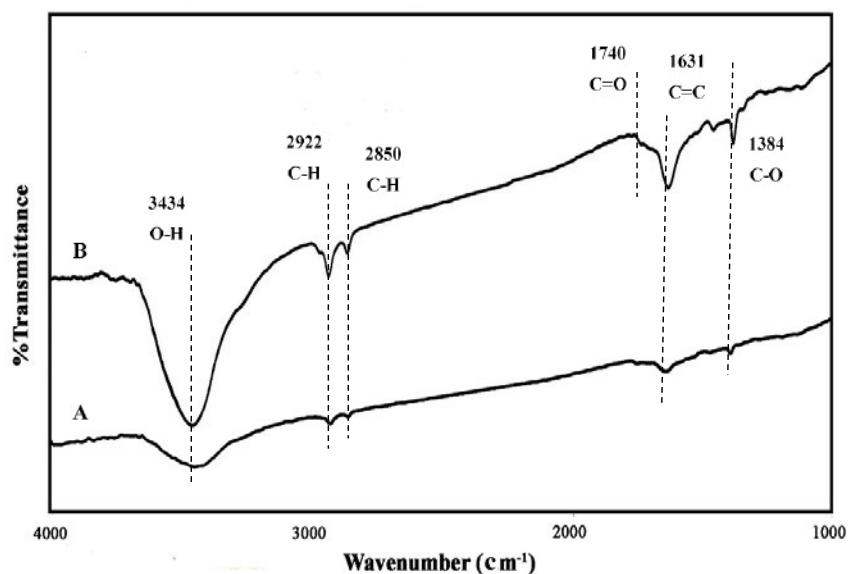


Fig. 1. FT-IR spectra of: A) pristine MWCNTs, and B) MWCNTs-COOH

in the range 4000–1000 cm^{-1} were recorded. For the pristine MWCNTs, the peak at 1629 cm^{-1} can be attributed to the (C=C) stretching, which indicates the graphite structure of MWCNTs [46].

Characteristic peaks of MWNTs-COOH observed at 1384 and 3434 cm^{-1} can be assigned to C-O and OH stretching vibrations of the carboxylic acid group, respectively [47]. The peak at 1631 cm^{-1} (C=C) indicates the graphite structure of MWCNTs-COOH, a new peak around 1740 cm^{-1} in the spectra of MWCNTs-COOH can be assigned to C=O stretching of the carboxylic acid groups [47]. The peaks at 2850 and 2922 cm^{-1} can be attributed to asymmetric and symmetric CH_2 stretching [46]. As compared with the FT-IR spectrum of pristine MWCNTs, results suggest that the carboxylic acid groups have been successfully introduced onto the surfaces of MWCNTs by acid treatment.

Fig. 2 shows XRD patterns of the pristine MWCNTs (Fig. 2-A) and MWCNTs-COOH (Fig. 2-B). The pristine MWCNTs samples revealed the presence of two diffraction peaks at 2θ values of 25.94° and 44.42° attributed to the graphite structure (002) and (100) planes of the MWCNTs, respectively [48]. No drastic change in the position of characteristic peaks of MWCNTs-COOH was observed, which suggests that MWCNTs are maintained with their original structure after the functionalization process with the carboxylic acid

groups.

SEM images for MWCNTs-COOH, CPE and MWCNTs-COOH/CPE are shown in Fig. 3. The acid treatment can fragment the MWCNTs and it can be seen that the MWCNTs-COOH are shorter in length (Fig. 3-A) [47]. The surface of CPE is shown in (Fig. 3-B), a layer of irregular and isolated flakes of graphite powder present on the surface of CPE. After MWCNTs-COOH were added to the paste matrix, it can be seen that MWCNTs-COOH were distributed on the surface of the electrode with special three-dimensional structure (Fig. 3-C), indicating that the MWCNTs-COOH were successfully modified on the CPE and observed morphology was in agreement with previous works [49-51].

Electrochemical behaviour of GA on MWCNTs-COOH/CPE

In order to study the electrocatalytic activity (behaviour) of GA on MWCNTs-COOH/CPE, DPV technique was used due to its low background currents. Fig. 4 shows the DPVs of different electrodes recorded in 0.2 M PBS, pH 2.0 at the scan rate of 0.148 Vs^{-1} . As shown in Fig. 4-a, in the absence of GA no obvious oxidation peak observed indicating that MWCNTs-COOH has no response in the absence of GA and the background current is very low. In the presence of GA (33 μM) two anodic

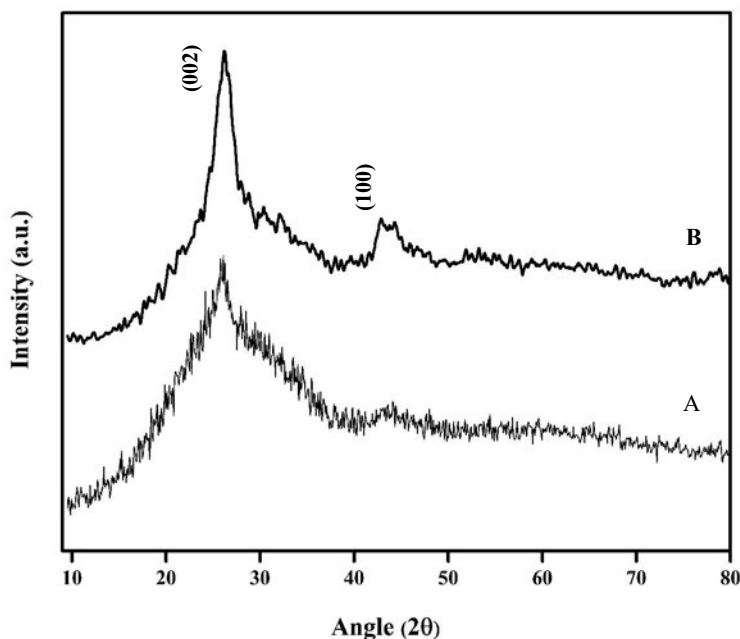


Fig. 2. XRD spectra of: A) pristine MWCNTs, and B) MWCNTs-COOH

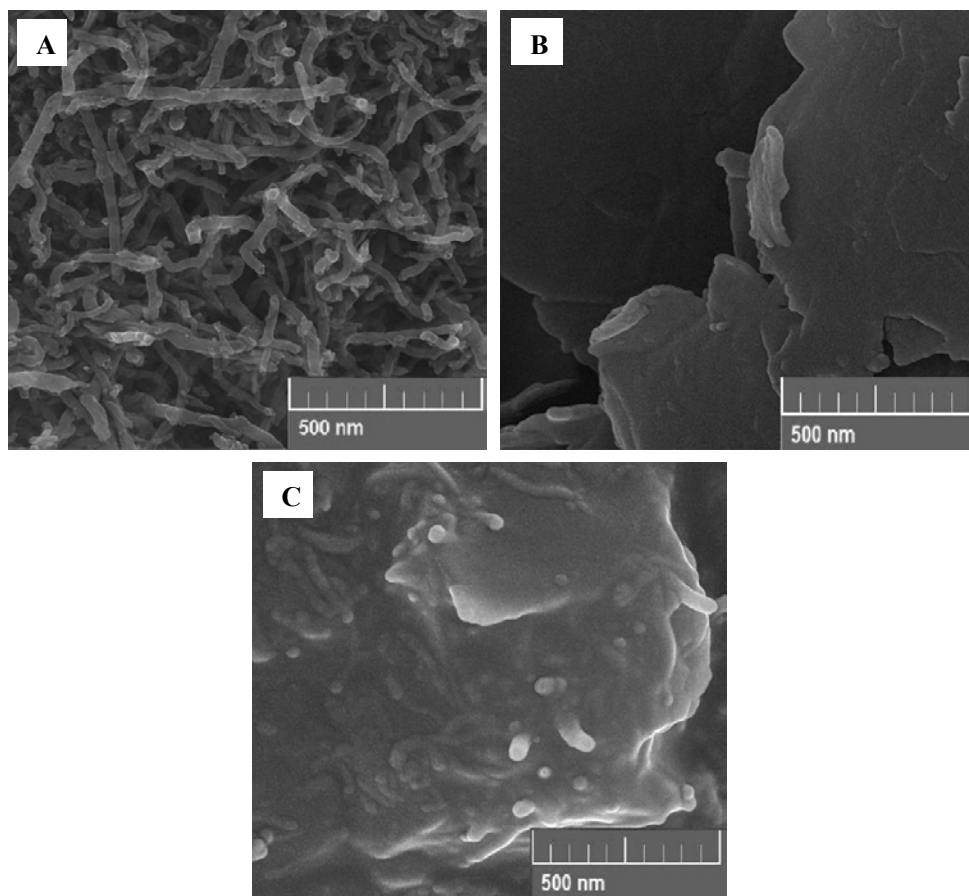


Fig. 3. SEM images of: A) MWCNTs-COOH, B) CPE, and C) MWCNTs-COOH/CPE

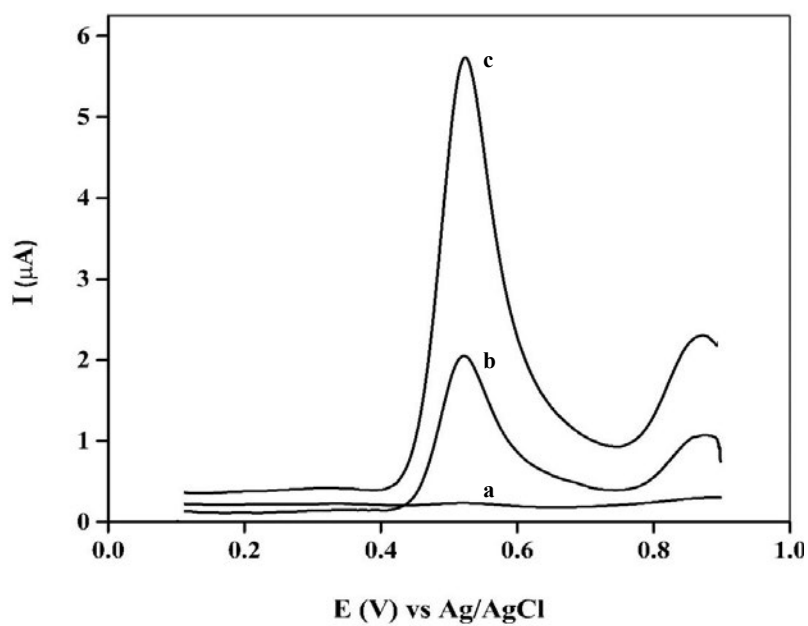


Fig. 4. DPVs of a) bare CPE in 0.2 M PBS (pH 2.0), b) bare CPE, and c) MWCNTs-COOH/CPE in 0.2 M PBS (pH 2.0) containing 33 μM GA at a scan rate of 0.148 Vs^{-1}

peaks around 0.5 and 0.8 V appeared on CPE (Fig. 4-b) and MWCNT-COOH/CPE (Fig. 4-c). The first peak is originated from semiquinone radical formation, followed by its oxidation to the quinone form (second peak) [52]. The second peak is very poor in comparison with the first one; hence we focused on the first oxidation peak for study GA oxidation. The response of MWCNTs-COOH/CPE toward electrooxidation of GA increases 3 times compared with the CPE. The enhanced catalytic activity of MWCNTs-COOH/CPE is due to unique properties such as high electrical conductivity and large surface area of MWCNTs.

The process of GA oxidation is affected by protonation reactions [42]. Thus, the influence of pH value of supporting electrolyte solution on the oxidation of GA at the MWCNTs-COOH/CPE surface studied using DPV. Through the increase in pH value from 2.0 to 5.0 at a scan rate of 0.148 Vs^{-1} , the peak current is reduced and the peak potential slightly shifted to more negative values, because the oxidation process of GA is related to H^+ ions of buffer solution [41]. The highest peak current was obtained at a pH of 2.0 (the results not shown here). Therefore, further studies were carried out at this pH value of the buffer solution.

Effect of potential scan rate

The effect of potential scan rate on MWCNTs-COOH/CPE in the electrooxidation of GA was studied by recording the CVs of a $33 \mu\text{M}$ GA in 0.2 M PBS, (pH 2.0) at scan rates of 0.027, 0.037, 0.047, 0.067, 0.087, 0.118, and 0.148 Vs^{-1} (Fig. 5). The oxidation peak currents of GA increased with increasing the potential scan rates and the anodic peak potential was shifted to the negative side. Inset shows that the oxidation peak current of GA was linear with the scan rate (ν), and the regression equation was $I_p = 0.0071 \nu + 1.0239$ (I_p : μA , ν : mVs^{-1} , $R^2 = 0.997$), indicating that the oxidation of GA at MWCNTs-COOH/CPE was controlled by the adsorption process [53].

Quantification of GA in MWCNTs-COOH/CPE

The DPVs of different concentrations of GA from 0.33 to $190 \mu\text{M}$ on MWCNTs-COOH/CPE is shown in Fig. 6. The sharp oxidation peaks observed and the peak current increased with increasing the concentration of GA. The calibration curve was made by plotting the current density of anodic peak versus the concentration of GA. The result was two range of linear calibration plots of low concentration (0.33 to $19.9 \mu\text{M}$; Fig. 6-A) and

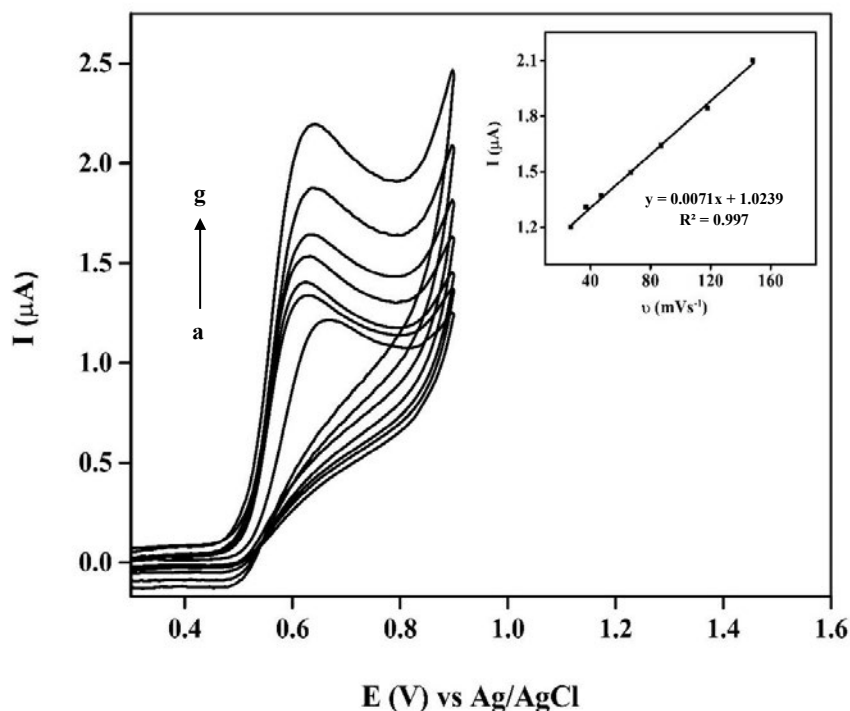


Fig. 5. CVs of MWCNTs-COOH/CPE in 0.2 M PBS (pH 2.0) containing $33 \mu\text{M}$ GA at scan rates of 0.027, 0.037, 0.047, 0.067, 0.087, 0.118 and 0.148 Vs^{-1} (a to g). Inset: the relationship between anodic peak current vs. potential scan rate

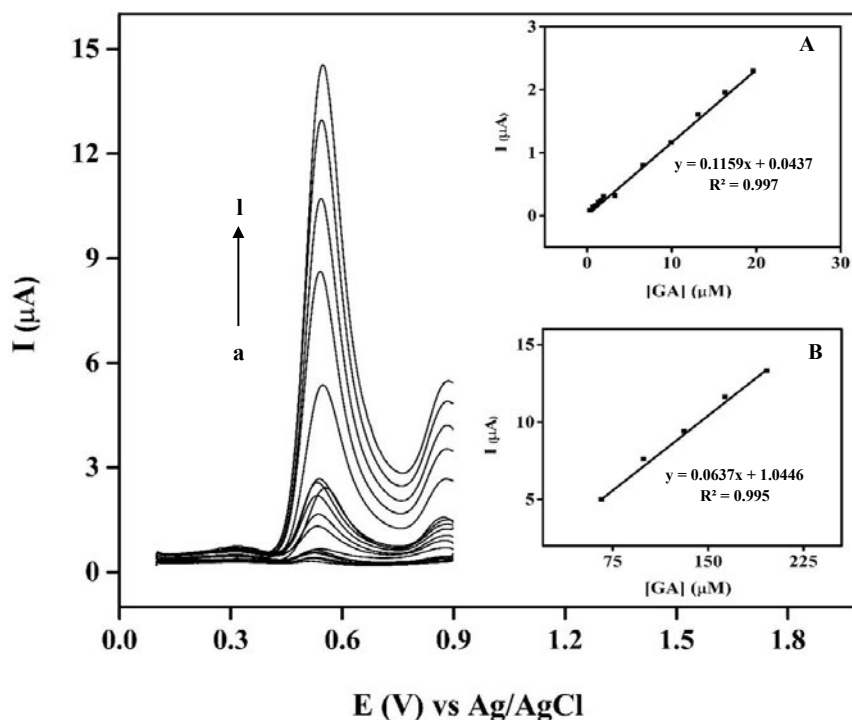


Fig. 6. DPVs of MWCNTs-COOH/CPE in 0.2 M PBS (pH 2.0) containing 0.33, 0.66, 0.99, 1.31, 1.96, 3.3, 6.6, 9.9, 13.1, 19.6, 66, 99, 131, 163 and 196 μM of GA at scan rate of 0.148 Vs^{-1} . Insets: relationship between the oxidation peak current and concentrations of GA in the range of A) 0.33 to 19.6 μM , and B) 66 to 196 μM

Table 1. Comparative results of the electrochemical GA detection on various electrodes

Electrode	Nanomaterial	Linear range (M)	Detection limit (M)	Ref.
GCE	Au microclusters/sulfonate functionalized graphene	$5.0 \times 10^{-8} - 8.0 \times 10^{-6}$	10.7×10^{-9}	54
CPE	Molecularly imprinted polymer-MWCNT	$0.12 \times 10^{-6} - 38.0 \times 10^{-5}$	47.0×10^{-9}	55
CPE	Graphene nanosheets	$3.0 \times 10^{-5} - 1.5 \times 10^{-4}$	1.1×10^{-7}	56
GCE	AgNP/delphinidin	$0.6 \times 10^{-6} - 6.2 \times 10^{-4}$	0.28×10^{-6}	57
GCE	Polyepinephrine	$1.0 \times 10^{-6} - 20.0 \times 10^{-6}$	6.63×10^{-7}	58
CPE	MWCNTs-COOH	$3.3 \times 10^{-7} - 1.9 \times 10^{-4}$	17.2×10^{-9}	This work

high concentration (66 to 190 μM ; Fig. 6-B). The regression equation of the calibration plot for high concentration of GA (CGA) was $I_p (\mu\text{A}) = 0.0637 \text{ CGA } (\mu\text{M}) + 1.0446$, ($R^2 = 0.995$) and for low concentration of GA was $I_p (\mu\text{A}) = 0.1159 \text{ CGA } (\mu\text{M}) + 0.0437$, ($R^2 = 0.997$) with the detection limit ($S/N=3$) of 17.2 nM. In Table 1 the ability of the proposed sensor for GA determination with some other sensors has been compared. As results of the comparison, this work suggests a simple, inexpensive, sensitive, and reliable sensor for GA determination and the proposed biosensor can be used as an analyzer device for estimation of total polyphenols of plant samples.

Real sample analysis

The presence of GA has been reported in *C. sinensis*, *V. odorata*, *C. wightii*, and *V. agnus-castus*. Standard addition method used for determination of GA in plant extracts. The DPVs of the standard addition method for the determination and measurement of GA in *C. sinensis*, *V. odorata*, *C. wightii*, and *V. agnus-castus* are shown in Figs. 7 to 10, respectively. Clear oxidation peak of each sample in the absence of GA appeared around 0.5 V (curve a in Figs. 7 to 10). After adding a certain amount of GA standard solution, the peak current at the same oxidation potential increased (curves b to e). Insets show the calibration curves resulted

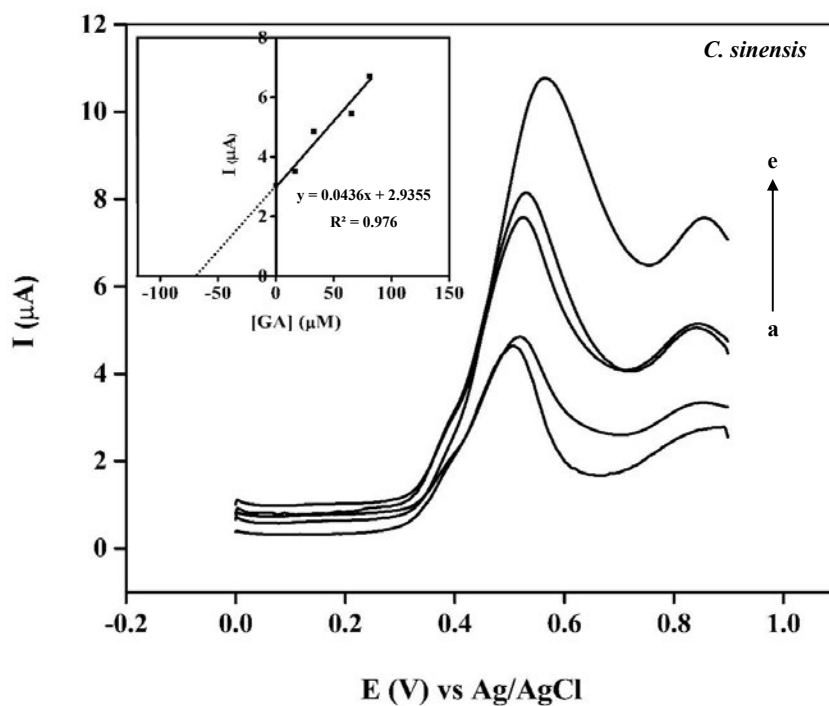


Fig. 7. DPVs of MWCNTs-COOH/CPE in 0.2 M PBS (pH 2.0) containing a) appropriate amounts of *C. sinensis* and b-e) increasing amounts of GA standard solution at a scan rate of 0.148 Vs^{-1} . Inset shows the corresponding standard addition curve for determination of GA in *C. sinensis*.

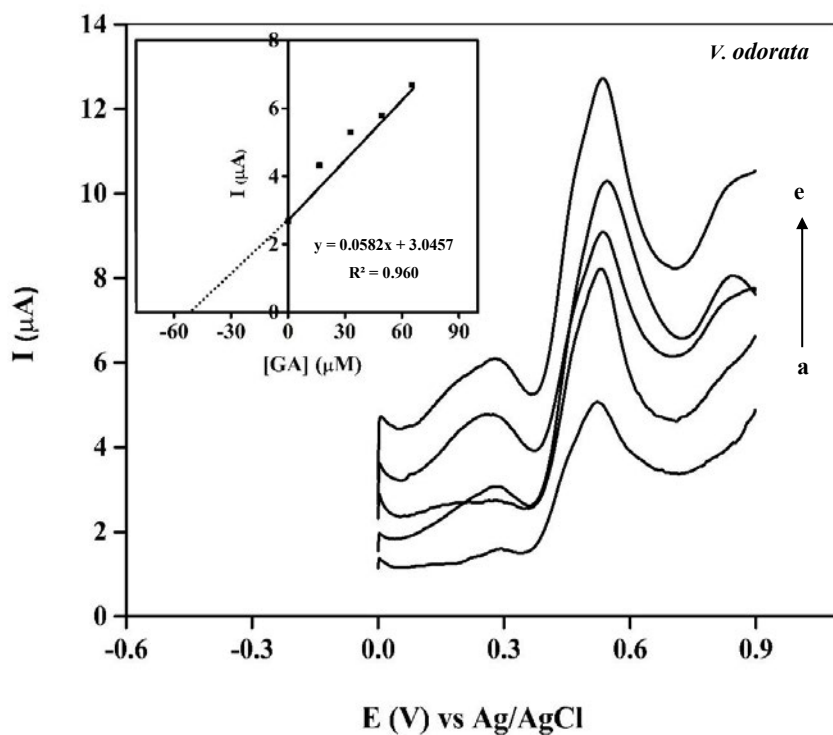


Fig. 8. DPVs of MWCNTs-COOH/CPE in 0.2 M PBS (pH 2.0) containing a) appropriate amounts of *V. odorata* and b-e) increasing amounts of GA standard solution at a scan rate of 0.148 Vs^{-1} . Inset shows the corresponding standard addition curve for determination of GA in *V. odorata*.

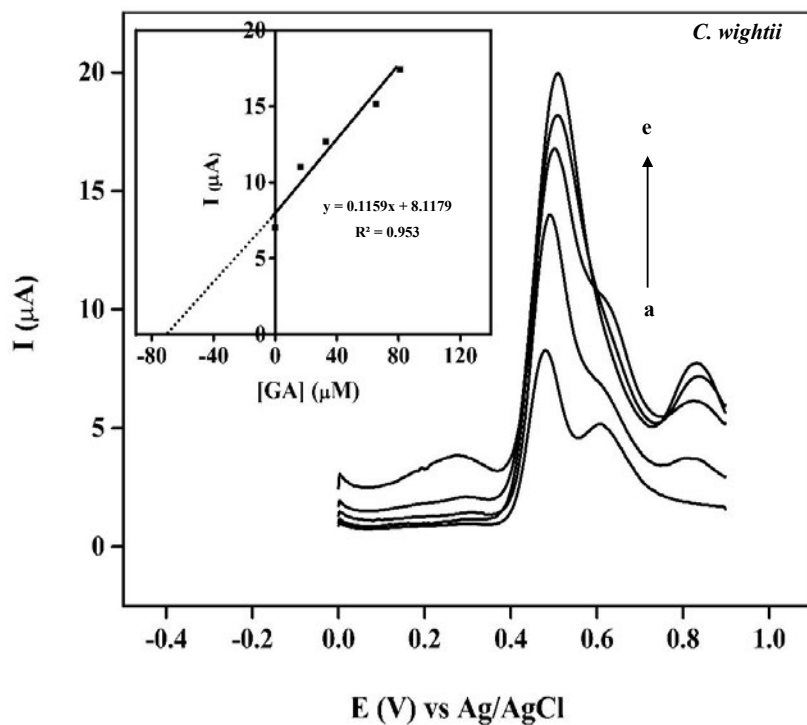


Fig. 9. DPVs of MWCNTs-COOH/CPE in 0.2 M PBS (pH 2.0) containing a) appropriate amounts of *C. wightii* and b-e) increasing amounts of GA standard solution at a scan rate of 0.148 Vs^{-1} . Inset shows the corresponding standard addition curve for determination of GA in *C. wightii*.

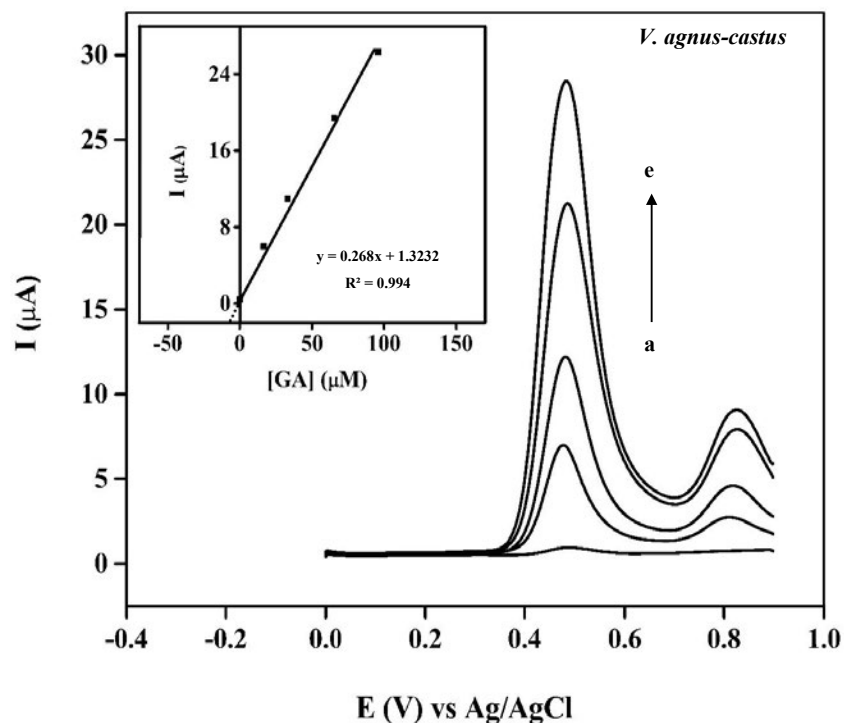


Fig. 10. DPVs of MWCNTs-COOH/CPE in 0.2 M PBS (pH 2.0) containing a) appropriate amounts of *V. agnus-castus* and b-e) increasing amounts of GA standard solution at a scan rate of 0.148 Vs^{-1} . Inset shows the corresponding standard addition curve for determination of GA in *V. agnus-castus*.

from standard edition DPVs of each sample. By extrapolating the calibration curve to $y=0$, the content of GA in extracts of *C. sinensis*, *V. odorata*, *C. wightii*, and *V. agnus-castus* estimated to be 11.4, 8.9, 11.91 and 2.9 mg L⁻¹, respectively.

CONCLUSION

In this paper, the MWCNTs-COOH/CPE was fabricated with a simple and low-cost method than used for fast, sensitive, and selective GA determination. Via Cyclic voltammetry and differential pulse voltammetry techniques, the MWCNTs-COOH/CPE represented great electrochemical effects toward GA oxidation. A good linear relationship of peak currents with the concentrations of GA ranging from 0.33 to 196 μ M and a low detection limit of 17.2 nM ($S/N = 3$) were obtained. Then, the sensor was successfully applied for the determination of GA content in *C. sinensis*, *V. odorata*, *C. wightii*, and *V. agnus-castus* extracts using the standard addition method.

ACKNOWLEDGEMENTS

Authors appreciate the support from the Council of the University of Kashan for providing financial support to undertake this work.

CONFLICT OF INTEREST

There is no conflict of interest associated with this work.

REFERENCES

- Pham-Huy LA, He H, Pham-Huy C. Free radicals, antioxidants in disease and health. *Int. J. Biomed. Sci.*, 2008; 4(2): 89-96.
- Ames B. Dietary carcinogens and anticarcinogens. Oxygen radicals and degenerative diseases. *Science*. 1983;221(4617):1256-64.
- Rice-Evans C, Miller N, Paganga G. Antioxidant properties of phenolic compounds. *Trends in Plant Science*. 1997;2(4):152-9.
- Collins PB, Thompson MA. Handbook on gallic acid: Natural occurrences, antioxidant properties and health implications. Nova Science Publisher's, Incorporated; 2013.
- Marques V, Farah A. Chlorogenic acids and related compounds in medicinal plants and infusions. *Food Chemistry*. 2009;113(4):1370-6.
- Erdogan Orhan I, Senol FS, Aslan Erdem S, Tatli II, Kartal M, Alp S. Tyrosinase and Cholinesterase Inhibitory Potential and Flavonoid Characterization of *Viola odorata* L. (Sweet Violet). *Phytotherapy Research*. 2015;29(9):1304-10.
- Rajani M, Bagul MS, Srinivasa H, Kanaki NS. Antiinflammatory activity of two Ayurvedic formulations containing guggul. *Indian Journal of Pharmacology*. 2005;37(6):399.
- Maltaş E, Uysal A, Yildiz S, Durak Y. Evaluation of antioxidant and antimicrobial activity of *Vitex agnus-castus* L. *Fresen. Environ. Bull.*, 2010; 19: 3094-3099.
- Kilmartin PA, Zou H, Waterhouse AL. A Cyclic Voltammetry Method Suitable for Characterizing Antioxidant Properties of Wine and Wine Phenolics. *Journal of Agricultural and Food Chemistry*. 2001;49(4):1957-65.
- Fujiki H, Watanabe T, Sueoka E, Rawangkan A, Suganuma M. Cancer prevention with green tea and its principal constituent, EGCG: From early investigations to current focus on human cancer stem cells. *Mol. Cells*, 2018; 41(2): 73-82.
- Bertipaglia de Santana M, Mandarino MG, Cardoso JR, Dichi I, Dichi JB, Camargo AEI, et al. Association between soy and green tea (*Camellia sinensis*) diminishes hypercholesterolemia and increases total plasma antioxidant potential in dyslipidemic subjects. *Nutrition*. 2008;24(6):562-8.
- Wang Q, Zhang J, Li Y, Shi H, Wang H, Chen B, et al. Green tea polyphenol epigallocatechin-3-gallate increases atherosclerotic plaque stability in apolipoprotein E-deficient mice fed a high-fat diet. *Kardiologia Polska*. 2018;76(8):1263-70.
- Barroso H, Ramalheite R, Domingues A, Maci S. Inhibitory activity of a green and black tea blend on *Streptococcus mutans*. *Journal of Oral Microbiology*. 2018;10(1):1481322.
- Fechtner S, Singh A, Chourasia M, Ahmed S. Molecular insights into the differences in anti-inflammatory activities of green tea catechins on IL-1 β signaling in rheumatoid arthritis synovial fibroblasts. *Toxicology and Applied Pharmacology*. 2017;329:112-20.
- Fassina G, Buffa A, Benelli R, Varnier OE, Noonan DM, Albini A. Polyphenolic antioxidant (–)-epigallocatechin-3-gallate from green tea as a candidate anti-HIV agent. *AIDS*. 2002;16(6):939-41.
- Hara Y, Yang CS, Isemura M, Tomita I. Health benefits of green tea: An evidence-based approach. CABI, 2017.
- Su Y-L, Cheng S-H. Sensitive and selective determination of gallic acid in green tea samples based on an electrochemical platform of poly(melamine) film. *Analytica Chimica Acta*. 2015;901:41-50.
- Yao L, Jiang Y, Datta N, Singanusong R, Liu X, Duan J, et al. HPLC analyses of flavanols and phenolic acids in the fresh young shoots of tea (*Camellia sinensis*) grown in Australia. *Food Chemistry*. 2004;84(2):253-63.
- Mousavi SH, Naghizade B, Pourgonabadi S, Ghorbani A. Protective effect of *Viola tricolor* and *Viola odorata* extracts on serum/glucose deprivation-induced neurotoxicity: role of reactive oxygen species. *Avicenna J. Phytomed.*, 2016; 6(4): 434-441.
- Vishal A, Parveen K, Pooja S, Kannappan N, Kumar S. Diuretic, laxative and toxicity studies of *Viola odorata* aerial parts. *Pharmacologyonline*, 2009; 1: 739-748.
- Gautam SS, Bithel N, Kumar S, Painuly D, Singh J. A new derivative of ionone from aerial parts of *Viola odorata* Linn. and its antibacterial role against respiratory pathogens. *Clinical Phytoscience*. 2016;2(1).
- Koochek MH, Pipelzadeh MH, Mardani H. The Effectiveness of *Viola odorata* in the Prevention and Treatment of Formalin-Induced Lung Damage in the Rat. *Journal of Herbs, Spices & Medicinal Plants*. 2003;10(2):95-103.
- Tania P, Chandra SA, H KK. Antioxidant and free radical scavenging activities of *Viola odorata* in the search of potential inhibitor of tobacco free radicals. *Journal of*

- Medicinal Plants Research. 2017;11(27):433-8.
24. Gontova TM, Mashtaler VV. Identification of flavanoids in thick extracts of *violet's* herb and hybrid *violet's* herb by HPLC method. Electronic Archive of the National Pharmaceutical University (Kharkov, Ukraine), 2016; 1: 49-53.
 25. Bellamkonda R, Rasineni K, Singareddy SR, Kasetti RB, Pasurla R, Chippada AR, et al. Antihyperglycemic and antioxidant activities of alcoholic extract of *Commiphora mukul* gum resin in streptozotocin induced diabetic rats. *Pathophysiology*. 2011;18(4):255-61.
 26. Madasu C, Gudem S, Sistla R, Uppuluri VM. Synthesis and anti-inflammatory activity of some novel pyrimidine hybrids of myrrhanone A, a bicyclic triterpene of *Commiphora mukul* gum resin. *Monatshefte für Chemie - Chemical Monthly*. 2017;148(12):2183-93.
 27. Lokhande PD, Jagdale SC, Chabukswar AR. Natural remedies for heart diseases. *Indian J. Tradit. Know.*, 2006; 5(3): 420-427.
 28. Babu K, Muguli G, Rao Vadaparthi PR, Ramesh B, Gowda V, Paramesh R, et al. A novel high-performance liquid chromatography-electron spray ionization-mass spectrometry method for simultaneous determination of guggulsterones, piperine and gallic acid in *Triphala guggulu*. *Pharmacognosy Magazine*. 2015;11(42):66.
 29. Wollenweber E, Mann K. Flavonols from fruits of *Vitex agnus castus*. *Planta Med.*, 1983; 48(2): 126-127.
 30. Sağlam H, Pabuçcuoğlu A, Kivçak B. Antioxidant activity of *Vitex agnus-castus* L. extracts. *Phytotherapy Research*. 2007;21(11):1059-60.
 31. Stojković D, Soković M, Glamočlija J, Džamić A, Ćirić A, Ristić M, et al. Chemical composition and antimicrobial activity of *Vitex agnus-castus* L. fruits and leaves essential oils. *Food Chemistry*. 2011;128(4):1017-22.
 32. Choudhary MI, Azizuddin, Jalil S, Nawaz SA, Khan KM, Tareen RB, et al. Antiinflammatory and lipooxygenase inhibitory compounds from *vitex agnus-castus*. *Phytotherapy Research*. 2009;23(9):1336-9.
 33. Sarikurkcı C, Arısoy K, Tepe B, Cakir A, Abali G, Mete E. Studies on the antioxidant activity of essential oil and different solvent extracts of *Vitex agnus castus* L. fruits from Turkey. *Food and Chemical Toxicology*. 2009;47(10):2479-83.
 34. Ismail A, Syahida Ramlı N, Mohamed M, Wan Ahmad WAN. Acute and Sub-Acute Antihypertensive Effects of *Syzygium polyanthum* Leaf Extracts with Determination of Gallic Acid using HPLC Analysis. *Pharmacognosy Journal*. 2018;10(4):663-71.
 35. Seo S-Y, Kang W. Quantitative determination of a synthetic amide derivative of gallic acid, SG-HQ2, using liquid chromatography tandem mass spectrometry, and its pharmacokinetics in rats. *Journal of Pharmaceutical and Biomedical Analysis*. 2016;131:103-6.
 36. Li S, Sun H, Wang D, Qian L, Zhu Y, Tao S. Determination of Gallic Acid by Flow Injection Analysis Based on Luminol-AgNO₃-Ag NPs Chemiluminescence System. *Chinese Journal of Chemistry*. 2012;30(4):837-41.
 37. Andreu-Navarro A, Fernández-Romero JM, Gómez-Hens A. Determination of antioxidant additives in foodstuffs by direct measurement of gold nanoparticle formation using resonance light scattering detection. *Analytica Chimica Acta*. 2011;695(1-2):11-7.
 38. Liu HX, Liu Q, Dong YJ, Huan YF, Wang LT, Ye KQ, et al. Determination of Gallic Acid Content in *Paeonia lactiflora* Pall by Capillary Zone Electrophoresis. *Advanced Materials Research*. 2013;850-851:1271-4.
 39. Pisoschi AM, Cimpeanu C, Predoi G. Electrochemical Methods for Total Antioxidant Capacity and its Main Contributors Determination: A review. *Open Chemistry*. 2015;13(1).
 40. Sangeetha NS, Narayanan SS. A novel bimediator amperometric sensor for electrocatalytic oxidation of gallic acid and reduction of hydrogen peroxide. *Analytica Chimica Acta*. 2014;828:34-45.
 41. Luo JH, Li BL, Li NB, Luo HQ. Sensitive detection of gallic acid based on polyethyleneimine-functionalized graphene modified glassy carbon electrode. *Sensors and Actuators B: Chemical*. 2013;186:84-9.
 42. Souza LP, Calegari F, Zarbin AJG, Marcolino-Júnior LH, Bergamini MrF. Voltammetric Determination of the Antioxidant Capacity in Wine Samples Using a Carbon Nanotube Modified Electrode. *Journal of Agricultural and Food Chemistry*. 2011;59(14):7620-5.
 43. Ince Yardimci A, Tanoglu M, Selamet Y. Development of electrically conductive and anisotropic gel-coat systems using CNTs. *Progress in Organic Coatings*. 2013;76(6):963-5.
 44. Ziyatdinova GK, Romashkina SA, Ziganshina ER, Budnikov HC. Voltammetric Determinations of Thymol on an Electrode Modified by Coimmobilized Carboxylated Multiwalled Carbon Nanotubes and Surfactants. *Journal of Analytical Chemistry*. 2018;73(1):63-70.
 45. Karimi S, Ghourchian H, Rahimi P, Rafiee-Pour H-A. A nanocomposite based biosensor for cholesterol determination. *Analytical Methods*. 2012;4(10):3225.
 46. Sadegh H, Zare K, Maazinejad B, Shahryari-ghoshekandi R, Tyagi I, Agarwal S, et al. Synthesis of MWCNT-COOH-Cysteamine composite and its application for dye removal. *Journal of Molecular Liquids*. 2016;215:221-8.
 47. Avilés F, Cauch-Rodríguez JV, Moo-Tah L, May-Pat A, Vargas-Coronado R. Evaluation of mild acid oxidation treatments for MWCNT functionalization. *Carbon*. 2009;47(13):2970-5.
 48. Sadegh H, Shahryari-ghoshekandi R, Kazemi M. Study in synthesis and characterization of carbon nanotubes decorated by magnetic iron oxide nanoparticles. *International Nano Letters*. 2014;4(4):129-35.
 49. Ajayan PM, Ebbesen TW, Ichihashi T, Iijima S, Tanigaki K, Hiura H. Opening carbon nanotubes with oxygen and implications for filling. *Nature*. 1993;362(6420):522-5.
 50. Keyvanfar M, Sami S, Karimi-Maleh H, Alizad K. Electrocatalytic determination of cysteamine using multiwall carbon nanotube paste electrode in the presence of 3,4-dihydroxycinnamic acid as a homogeneous mediator. *Journal of the Brazilian Chemical Society*. 2013;24(1):32-9.
 51. Ensafi AA, Karimi-Maleh H, Mallakpour S. N-(3,4-Dihydroxyphenethyl)-3,5-dinitrobenzamide-Modified Multiwall Carbon Nanotubes Paste Electrode as a Novel Sensor for Simultaneous Determination of Penicillamine, Uric acid, and Tryptophan. *Electroanalysis*. 2011;23(6):1478-87.
 52. Petković BB, Stanković D, Milčić M, Sovilj SP, Manojlović D. Dinuclear copper(II) octaazamacrocyclic complex in a PVC coated GCE and graphite as a voltammetric sensor for determination of gallic acid and antioxidant capacity of wine samples. *Talanta*. 2015;132:513-9.

53. Laviron E. A multilayer model for the study of space distributed redox modified electrodes Part II. Theory and application of linear potential sweep voltammetry for a simple reaction. *Journal of Electroanalytical Chemistry*. 1980;112(1):11-23.
54. Liang Z, Zhai H, Chen Z, Wang H, Wang S, Zhou Q, et al. A simple, ultrasensitive sensor for gallic acid and uric acid based on gold microclusters/sulfonate functionalized graphene modified glassy carbon electrode. *Sensors and Actuators B: Chemical*. 2016;224:915-25.
55. Shojaei S, Nasirizadeh N, Entezam M, Koosha M, Azimzadeh M. An Electrochemical Nanosensor Based on Molecularly Imprinted Polymer (MIP) for Detection of Gallic Acid in Fruit Juices. *Food Analytical Methods*. 2016;9(10):2721-31.
56. Sheikh-Mohseni MA. Sensitive electrochemical determination of gallic acid: application in estimation of total polyphenols in plant samples. *Anal. Bioanal. Chem. Res.*, 2016; 3(2): 217-224.
57. Ghaani M, Nasirizadeh N, Yasini Ardakani SA, Mehrjardi FZ, Scampicchio M, Farris S. Development of an electrochemical nanosensor for the determination of gallic acid in food. *Analytical Methods*. 2016;8(5):1103-10.
58. Abdel-Hamid R, Newair EF. Adsorptive stripping voltammetric determination of gallic acid using an electrochemical sensor based on polyepinephrine/glassy carbon electrode and its determination in black tea sample. *Journal of Electroanalytical Chemistry*. 2013;704:32-7.